Int. J. Econ. Environ. Geol. Vol. 14 (1) 21-30, 2023

Journal home page: www.econ-environ-geol.org

Open Access

ISSN: 2223-957X

Appraisal of Neotectonic Activities in Shadi Kaur Catchment, Pasni, Balochistan-Pakistan

Waseem Khan [1*], Mahnoor Mirwani [2,3], Inayat Ullah [4], Aimal Khan Kasi [4], Muhammad Ishaq Kakar [4], Shazia Fareed [5]

[1] Guangdong Provincial Key Laboratory of Geodynamics and Geohazards, School of Earth Sciences and Engineering, Sun Yat-Sen University, Zhuhai, China

[2]Communication and Works, Physical and Housing Department, Government of Baluchistan, Pakistan

[3] Department of Civil Engineering, Balochistan University of Information Technology Engineering and Management Sciences, Quetta, Pakistan

[4]Centre of Excellence in Mineralogy, University of Balochistan, Quetta, Pakistan

[5] Department of Geology, University of Balochistan, Quetta, Pakistan

* Email: khanw@mail2.sysu.edu.cn

Received: *08 May, 2023* ***Accepted:*** *24 July, 2023*

The goal of this research is to assess Neotectonic activity in the northern Pasni region of Balochistan-Pakistan. For a total of 57 drainage sub-basins, four geomorphic parameters were calculated. These include the Factor of asymmetry (F_A), Shape of the Basin (S_B), Hypsometric Integral (*HI*), and Length Gradient of the stream (LG_S). The Index of Neotectonic (*IN*) was computed using a combination of the calculated geomorphic characteristics. The basins were then classified as having high, moderate, and low intensities as a result of this indexing. The tectonic strain by major lineation found between Hoshab fault and NNE trending Nai Rud fault and NNE trending Ghulaman-i-Bent fault, respectively, has influenced the mechanism of current channels geometry, according to the quantitative analysis. The *IN* intensities distribution revealed considerable disparities amongst drainage sub basins, indicating variances in Neotectonic activity due to their placement in relation to the study area's fault networks. A total of 8 knick points including the slope-break and vertical-step, were distinguished within the catchment area depending on the influencing factors.

Keywords: Geomorphic parameters, Shadi Kaur Catchment, Ghulaman-i-Bent Fault, Nai Rud Fault, Pasni, Balochistan

Introduction

In tectonically active areas, landscapes are formed when the effects of crustal block motion and surface processes like erosion and deposition interact. The interaction of climatic, tectonics and lithological conditions causes landscape change (Burbank and Anderson, 2012). As a result, landscape morphology can reveal the interplay between tectonics and surface phenomenon (Keller and Pinter, 2002). Streams arrangements play a key factor in the whole approach because they are both affected by and reflect tectonic conditions. Moreover, they are linked in the evolution of the Earth's surface topography and interpret tectonic circumstances (Karymbalis et al., 2016; Keller and Pinter, 2002; Vassilakis et al., 2007).

Pasni's landscapes show the impact of recent tectonics in a variety of ways. Morphotectonics, which includes the quantitative analysis of drainage networks and catchments, can help us learn more about active fault evolution in areas where historical earthquake data is scarce (Goldsworthy and Jackson, 2000). Quantitative data are used in these investigations, allowing geomorphologists to construct morphometric parameters that can help discover tectonic assessments. These methodologies provide a quantifiable technique to analyze the influence of tectonic activities on the evolution of landscape structure in a precise location (Karymbalis et al., 2018; Keller and Pinter, 2002).

A single quantitative analysis is applicable to determine the Neotectonic activities of particular region, nonetheless the accuracy increases when using multiple geomorphic parameters (el- Hamdouni et al., 2008; Keller and Pinter, 2002). Numerous analyses emphasis on one metric for a given region (Maroukian et al., 2008; Siddiqui and Soldati, 2014), but plenty use multiple quantitative morphometric factors to assess tectonic activity across a larger region (Crosby and Whipple, 2006; Dehbozorgi et al., 2010). In recent studies of active tectonics, measurement of drainage basin topography using a combination of different morphometric characteristics to construct one combine parameter which may be applied to define neotectonic activities has become popular (Khan et al., 2022; Anand and Pradhan, 2019; Arian and Aram, 2014; Dehbozorgi et al., 2010; el-Hamdouni et al., 2008; Mahmood and Gloaguen, 2012). Further, Knick point's identification is widely used to estimate the tectonic and climatic implications. In most coastal places, a stream in equilibrium has a concave up longitudinal profile, which allows it to burn the least amount of energy while moving toward base level, which is the ocean. A Knick point is a break in the gentle curvature that is frequently marked by a "convex reach" (Berlin and Anderson, 2007).

The Shadi Kaur Catchment is an active tectonic zone where the Nai Rud thrust fault exists to the south of the catchment and the strike-slip Hoshab fault to the north,

two of Balochistan's most active structural features. The impact of neotectonic activities on the region is unclear, and quantitative research using several geomorphic characteristics by combining them to form the Index of Neotectonic may proceed to a determination of the neotectonic intensities. Further, an effort is carried out to examine the Knick points, their types and consequences.

The Shadi Kaur Catchment contains a large volume of Oligocene to Recent age of sediments, which are structurally running E–W in the north and NNE alignment in the south (Fig. 1). The Oligocene-Miocene Panjgur Formation, Lower Miocene Parkini Mudstone, Upper Miocene Talar Formation, Quaternary, and Recent deposits are mostly found in the study area (Cheema et al., 1977; Hunting Survey Corporation, 1960). Within broad synclinal formations, the shallow marine younger sequences (i.e., Miocene to Holocene) were deposited which are twisted relics of separate basins caught between the accretionary ridges of the trench slope (Farhoudi and Karig, 1977). The Oligocene to Miocene deposit were formed on the marine floor of the Oman Gulf predecessor before being tectonically absorbed into the accretionary wedge. While, the Lower Miocene and onward sequences characterize slope and shelf materials formed on the wedge top (Harms et al., 1982; Harms et al., 1984). The formations and descriptions are shown in the caption of Fig. 1.

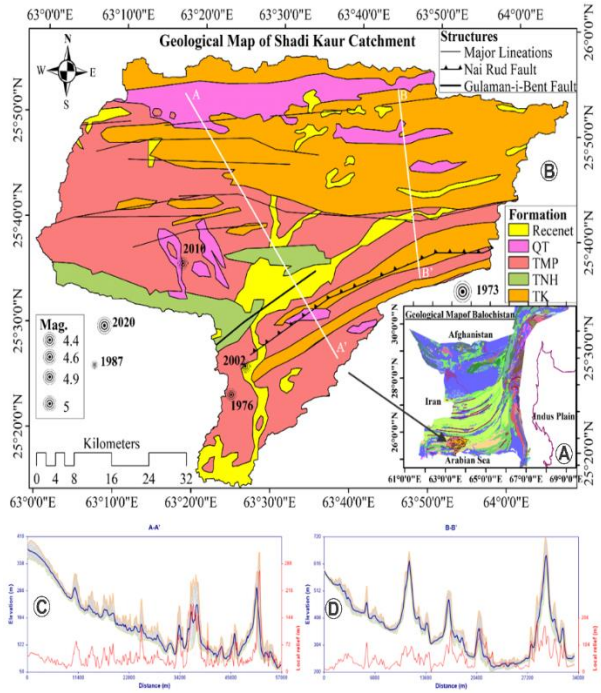

Fig. 1 Showing (A) the inset map showing the geological map of Balochistan-Pakistan (after, Khan and Mirwani, 2020; Khan et al., 2023a; Khan et al., 2023b), (B) the geological map of the Shadi Kaur Catchment, Pasni, Balochistan-Pakistan (after, Khan and Mirwani, 2020; Khan et al., 2023a; Khan et al., 2023b). (C) the cross-sectional elevation graphs of A-A' as shown in Fig. 1B, and (D) the cross-sectional elevation graphs of B-B' as shown in Fig. 1B. Where, QT: Quaternary alluvial deposits, TNH: Talar Formation (Upper Miocene; Cyclic succession of sandstones and shales), TMP: Parkini Mudstone (Lower Miocene; Mudstones with occasional sandstones), TK: Panjgur Formation (Oligocene to Early Miocene; Sandstone with interbedded claystone/shale).

More rapid sea floor spreading resumed in the Middle Miocene, and the Indian plate's continental lithosphere began to under thrust Eurasia. South of the Makran coast, subduction was reactivated. Folding and thrust faulting of the Makran flysch are the most visible signs of this alteration. There have been only two major faults identified in the catchment area including Nai Rud Fault and Ghulaman-i-Bent Fault. Apart from these two faults, numerous major lineation are present in the northern parts.

The Shadi Kaur Catchment occupies an area of about 13175.8 Km^2. The annual rainfall of the study area ranges from 111.10 to 138.52 mm increasing toward NE (Fig. 2) rainfall data after; (Harris et al., 2020). In addition, the rate of evaporation 1830 to 1930 mm which is higher than the rate of rainfall within the Shadi Kaur catchment (Kehl, 2009). The derived data (1920-2022) from USGS Earthquake Catalog show that only ten earthquakes occurred in offshore Pasni, while only three exist in the Catchment with no destruction greater than a magnitude of 5 (Fig. 1).

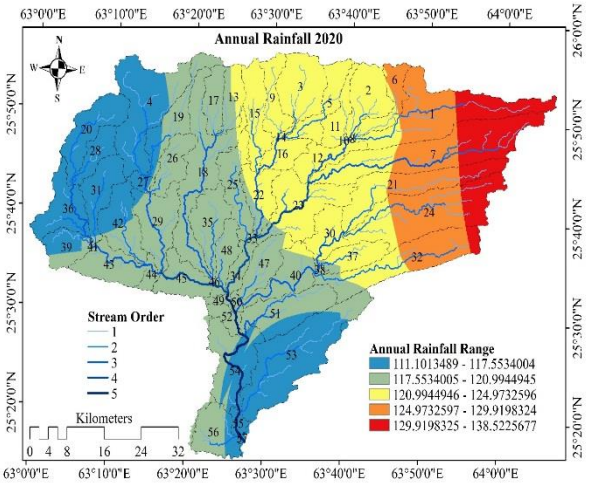

Fig. 2 Demonstrates the annual rainfall from 2011 to 2020, Shadi Kaur Catchment, Pasni, Balochistan-Pakistan (Harris et al., 2020).

Material and Methods

The digital elevation model (DEM) tiles of 30 m were mosaic by ArcGIS v. 10.5 for extracting the study area. Along with the Spatial Analyst tool, numerous ArcGIS extensions were used to examine the geomorphic parameters such as ArcHydro Toolbox for automatically extracting the sub basins, SLiX Toolbox to calculate SL index (Piacentini et al., 2020). In addition, the Matlab topo toolbox was performed to generate the Knick points.

Four geomorphic metrics, including Factor of Asymmetry (F_A), Shape of Basin (S_B), Hypsometric Integral (*HI*), and Length Gradient of Stream (LG_S) were estimated for a total of 57 sub basins to evaluate the landscapes change. The F_A and *HI* are often

utilized geomorphic parameters, and they are regarded basic reconnaissance indices for detecting tectonic deformation (Keller and Pinter, 2002). The Neotectonic intensities of the individual parameters were divided into 3 classes. The Class 1 represents high Neotectonic, Class 2 moderate activities, and Class 3 with low tectonics. These parameters were then combined to form the Index of Neotectonic (*IN*). The combined index was further categorized into 4 intensities. A series of maps depicting the spatial distribution of the values of these geomorphic parameters in the study region were generated in addition to the compilation of descriptive statistics for all of the basin indices.

The F_A metric is applied to determine if tectonics exists at the sub basin scale, and is formulated by:

$$FA = \left(\frac{Ar}{At}\right)100$$

Ar is the drainage basin to the right (downstream)

At is the drainage basin's entire area.

Under stable state where no significant tilting occurring in a catchment, the F_A is 50. Tilting due to lithological circumstances or Neotectonic variations in a watershed is indicated by indices above or below 50.

In active tectonic locations, the shape of young drainage basins is elongated, and run directly corresponding to the mountain's topographic slope. The elongated shape gradual changes into a circular shape by the absence of Neotectonic or erosional processes (Bull and McFadden, 1977).

$$SB = \frac{LB}{WB}$$

L_B denotes the basin length from the mouth to headwaters

W_B denotes the width at the broadest area of the basin

Higher S_B results, imply elongated basins with proportionally greater Neotectonic intensity, and lower S_B results designate with lesser neotectonic intensity.

The HI represents the elevation dispersion at certain geographic regions (Strahler, 1952). It was calculated with the help of the formula (Keller and Pinter, 2002; Mayer, 1990; Pike and Wilson, 1971):

$$HI = \frac{Hmean - Hmin}{Hmax - Hmin} \times 100$$

The mean elevation of the basin represents *Hmean*,

The lowest elevation of the basin represents *Hmin*,

The highest point represents *Hmax*.

High values more than 50, on average, indicate high topography with a hypsometric curve of convex. The moderate ratios between 40 to 50 reflect curves of concave-convex. Whereas, lower ratios less than 40, on average, indicate concave forms (Keller and Pinter, 2002). Lower ratios are associated with old landscapes which are less affected by neotectonic activities and excessive erosion. While the higher ratios signify higher Neotectonic activities and lower erosional processes.

The LG_S parameter denotes a dynamic equilibrium between erosion progressions for Instance Rivers and flow of stream. (Hack, 1973), neotectonic activity (Keller and Pinter, 2002), and may be applied to investigate neotectonic activities (el-Hamdouni et al., 2008). The formula is expressed as:

$$LGS = \left(\frac{\Delta H}{\Delta L}\right)L$$

Where, gradient or slope of the channel reach is denoted by $\Delta H/\Delta L$. The elevation change of reach is ΔH and length of the reach is ΔL. The total channel length is denoted by *L (*from the channel's highest point to the upstream midpoint of the reach of interest).

The LG_S can be used to assess correlations between topography, bedrock resistance and neotectonic activities. In an active uplift area where a channel flows, the LG_S increases, and it decreases where the channel flows parallel to specific features (Keller and Pinter, 2002).

The increased value imply that the landscape is not affected by erosion, and reflect a relatively young terrain, possibly caused by Neotectonic activities (el-Hamdouni et al., 2008).

To better improve the evaluation accuracy of neotectonic activities in the Shadi Kaur Catchment, the four examined parameters were merged and the mean classes yielded *IN*, which is determined from the equation:

$$IN = \frac{(FA + SB + HI + LGS)}{4}$$

Extreme 1.0 - ≤1.5 (1), high 1.0 - ≤1.5 (2), moderate ≥ 2.0 - ≤ 2.5 (3), and low ≥ 2.5 - ≤ 3.0 (4) tectonic activity were assigned to the drainage basins based on the *IN* values. To draw inferences about the tectonic pattern of the research area, an atlas illustrating the dispersal of *IN* intensities was created.

Stream profiles include information on climatic and /or geomorphological perturbations in the form of Knick points migrating upstream (Gilbert, 1877 and Mackin, 1948). Plotting ksn-values allows for the quantification of deviations from the logarithmic channel length profile, allowing for the detection and visualization of these sites in the stream network.

The stream power model of sediment transport/incision

is assumed to apply, i.e., sediment transport or incision are functions of the energy expenditure of water when moving downstream. The stream power model is written in the form below in the context of landscape evolution;

$$\frac{dz}{dt} = U - kA^m \left(\frac{dz}{dx}\right)^n$$

The uplift rate is U, the upslope area is A, the slope is dz/dx, and the coefficients are k, m, and n. The processes of uplift and incision are in equilibrium in steady state, with dz/dt=0 at each point along the profile. As a result, the equation has been rearranged.

$$\left(\frac{dz}{dx}\right)^n = \frac{U}{kA^m}$$

$$dzdt = Uk1/nA - n/m$$

The terms have been rewritten in such a way that

And

$$K_{sn} = \frac{S}{A^{-\theta}}$$

Where ksn and θ are the normalised channel steepness and channel concavity, respectively. θ varies from 0.3 to 0.8, with 0.45 being the most common value. It can be calculated using either slope-area plots or χ-plots (Kirby and Whipple, 2001; Tucker and Whipple, 2002; Whipple et al., 2013; Wobus et al., 2006).

Results and Discussion

The calculated Af results are shown in Table 1 and Figure 3A. The results are distributed into three classes. The results show 22 sub basins falling in Class 1 with an occupancy of 38.59%, Class 2 with 26.32%,

Table 1 The quantitative assessments of geomorphic parameters of the Shadi Kaur Catchment, Pasni at the coast of Balochistan-Pakistan.

Basin	H_I	Class	F_A	Class	S_B	Class	LGs	Class	IN Class	H_I Curve
1	0.48	2	0.46	3	3.04	2	742.10	1	2	Young
2	0.46	2	0.77	1	2.01	3	250.67	3	3	Mature
3	0.48	2	0.49	3	1.40	3	384.25	3	4	Mature
4	0.48	2	0.43	3	1.21	3	267.99	3	4	Old
5	0.47	2	0.59	2	3.14	2	417.99	3	3	Mature
6	0.46	2	0.66	1	3.28	2	588.35	2	2	Mature
7	0.46	2	0.65	1	6.87	1	875.61	1	1	Mature
8	0.41	2	0.38	2	1.18	3	n/a	n/a	3	Mature
9	0.48	2	0.37	2	2.03	3	458.92	3	3	Mature
10	0.37	3	0.23	1	1.82	3	n/a	n/a	3	Young
11	0.46	2	0.78	1	2.71	3	n/a	n/a	2	Old
12	0.49	2	0.75	1	2.53	3	328.08	3	3	Mature
13	0.49	2	0.77	1	2.75	3	n/a	n/a	2	Old
14	0.40	2	0.68	1	1.28	3	n/a	n/a	2	Young
15	0.48	2	0.44	3	3.87	2	463.95	3	3	Old
16	0.50	2	0.44	3	1.99	3	348.51	3	4	Mature
17	0.47	2	0.67	1	2.89	3	439.75	3	3	Old
18	0.47	2	0.52	3	4.03	1	444.95	3	3	Old
19	0.49	2	0.53	3	3.97	2	413.06	3	3	Old
20	0.49	2	0.60	2	3.50	2	212.89	3	3	Mature
21	0.48	2	0.69	1	5.38	1	536.54	2	1	Mature
22	0.48	2	0.55	3	1.69	3	275.41	3	4	Mature
23	0.47	2	0.54	3	1.70	3	317.06	3	4	Mature
24	0.48	2	0.26	1	3.72	2	350.49	3	2	Old
25	0.48	2	0.61	2	2.66	3	350.11	3	3	Young
26	0.48	2	0.37	2	2.19	3	293.44	3	3	Mature
27	0.50	2	0.42	2	1.65	3	n/a	n/a	3	Mature
28	0.48	2	0.48	3	2.54	3	n/a	n/a	4	Mature
29	0.47	2	0.79	1	1.55	3	159.33	3	3	Mature
30	0.46	2	0.47	3	0.93	3	192.43	3	4	Mature
31	0.47	2	0.56	3	2.35	3	220.08	3	4	Young
32	0.47	2	0.53	3	5.60	1	455.73	3	3	Mature
33	0.39	3	0.28	1	1.56	3	n/a	n/a	3	Old
34	0.47	2	0.50	3	3.08	2	n/a	n/a	3	Old
35	0.49	2	0.66	1	2.04	3	223.92	3	3	Mature
36	0.50	2	0.71	1	1.33	3	190.71	3	3	Young
37	0.47	2	0.37	2	3.20	2	190.92	3	3	Old
38	0.45	2	0.48	3	2.37	3	n/a	n/a	4	Young
39	0.44	2	0.71	1	1.02	3	n/a	n/a	2	Old
40	0.47	2	0.46	3	1.53	3	246.30	3	4	Mature
41	0.40	2	0.66	1	0.92	3	n/a	n/a	1	Mature
42	0.48	2	0.63	2	1.82	3	178.30	3	3	Mature
43	0.47	2	0.74	1	2.01	3	175.73	3	3	Old
44	0.45	2	0.50	3	1.21	3	n/a	n/a	4	Old

(Flint, 1974 and Howard, 1983);

$$S = K_{sn} A^{-\theta}$$

and Class 3 with 35.09%. While, the range of Af is from 0.23 (sub basin 10) to 0.80 (sub basin 57), and a mean AF of 0.53. This signifies approximately an equal distribution of all three classes. In fact, Class 1

45	0.49	2	0.52	3	1.44	3	n/a	n/a	4	Old
46	0.42	2	0.57	2	0.89	3	n/a	n/a	3	Old
47	0.48	2	0.41	2	2.19	3	185.85	3	3	Mature
48	0.46	2	0.37	2	2.40	3	154.26	3	3	Mature
49	0.46	2	0.35	2	3.03	2	n/a	n/a	2	Old
50	0.45	2	0.47	2	1.98	3	n/a	n/a	3	Mature
51	0.48	2	0.27	1	2.48	3	225.43	3	3	Old
52	0.46	2	0.63	2	1.49	3	n/a	n/a	3	Old
53	0.44	2	0.44	3	2.93	3	227.62	3	4	Old
54	0.45	2	0.67	1	1.24	3	156.53	3	3	Old
55	0.45	2	0.33	1	1.12	3	n/a	n/a	2	Old
56	0.48	2	0.43	3	0.81	3	121.26	3	4	Mature
57	0.31	3	0.80	1	1.07	3	n/a	n/a	3	Young
Mean	**0.46**	**2.05**	**0.53**	**1.96**	**2.33**	**2.68**	**326.07**	**2.84**	**2.98**	
Minimum	0.31	2	0.23	1	0.81	1	121.26	1	1	
Maximum	0.50	3	0.80	3	6.87	3	875.61	3	4	

resembling a great AF value with 22 sub basins out of 57, denoting low to high tectonic activities of the region.

The results SB are displayed in Table 1 and Figure 3B. Among the three classes of S_B, 4 sub basins acquiring 7.02% belong to Class 1, 10 sub basins resembling 17.54% belong to Class 2, and 43 sub basins consisting of 75.44% belong to Class 3. The values range from 0.81 (sub basin 56) to 6.87 (sub basin 7) with a mean value of 2.33. The results of BS show low tectonic activities in the area.

The examined HI results are shown in Table 1 and Figure 3C. There was no sub basin falling in Class 1, while Class 2 comprises 54 sub basins acquiring 94.74%, and Class 3 resembling 3 sub basins with an occupancy of 5.26%. The HI values range from 0.31 (sub basin 57) to 0.50 (sub basins 16, 27 and 36) with an average of 0.46. These results show moderate tectonic activities in the region. Moreover, the HI curves were applied to test the maturity of the sub basins Table 1, Figure 4. The curves show 35.09% (20 sub basins) belong to Old stage (monadnock phase), 50.88% (29 sub basins) belong to Mature stage (equilibrium phase), and 14.03% (8 sub basins) belong to Young stage (inequilibrium phase). This signifies monadnock to equilibrium phases of the area and denoting less tectonic activities in the region.

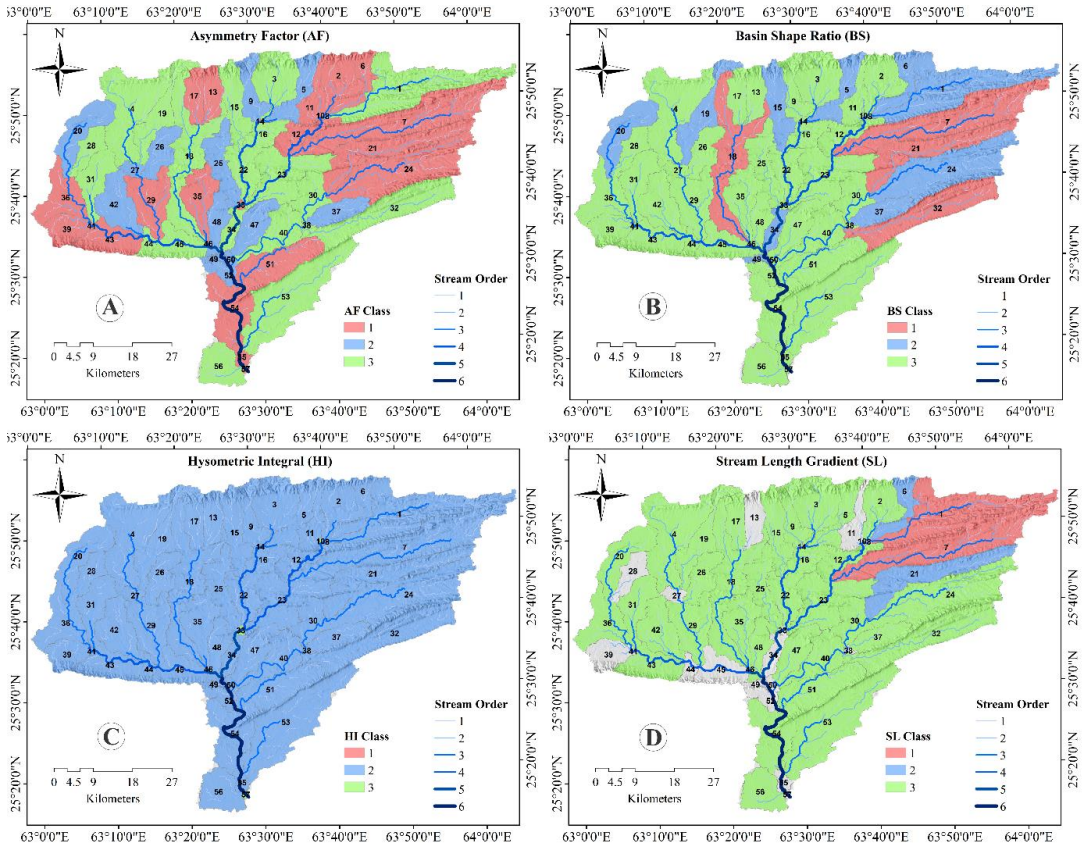

Fig. 3 Map showing the four calculated geomorphic parameters of the Shadi Kaur Catchment in Pasni at the coast of Balochistan, Pakistan (A) Factor of asymmetry, (B) shape of the basin (C) hypsometric integral, and (D) length gradient of stream. Note that the sub basins with no colors were not suitable to extract the SL index due to the threshold errors while calculating (D).

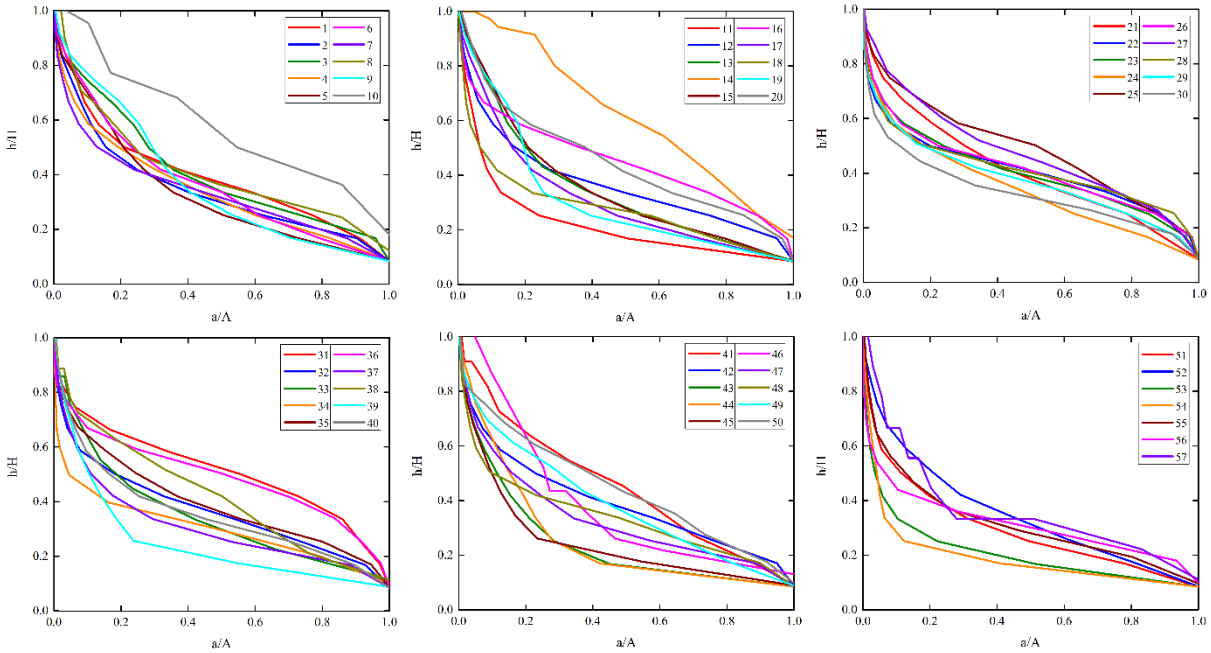

Fig. 4 Graphs illustrating the hypsometric curves of the sub basins of the Shadi Kaur Catchment, Pasni, Balochistan-Pakistan.

The calculated outcomes of LGs are shown in Table 1 and Figure 3D. Three classes were proposed to distinguish the LG_s scales. The Class 1 comprises 5.41% (2 sub basins), Class 2 acquires 5.41% (2 sub basins), and Class 3 resembles 89.18% (33 sub basins). While, 20 sub basins were not suitable to acquire the LG_S values. The acquired LG_S values range from 121.26 (sub basin 56) to 875.61 (sub basin 7) with a mean of 326.07. The LG_s index denotes low tectonic activities in the area.

The IN index was designed considering the above four geomorphic parameters and the results are shown in Table 1 and Figure 5. The index was categorized into four intensity classes. The Class 1 occupied 5.26% (3 sub basins) with extreme tectonic activities, Class 2 acquired 15.79% (9 sub basins) with high tectonic activities, Class 3 occupied 54.39% (31 sub basins) with moderate, and Class 4 occupied 24.56% (14 sub basins) low tectonic activities. Thus, the results of the IN index indicate moderate to low neotectonic activities in Shadi Kaur Catchment.

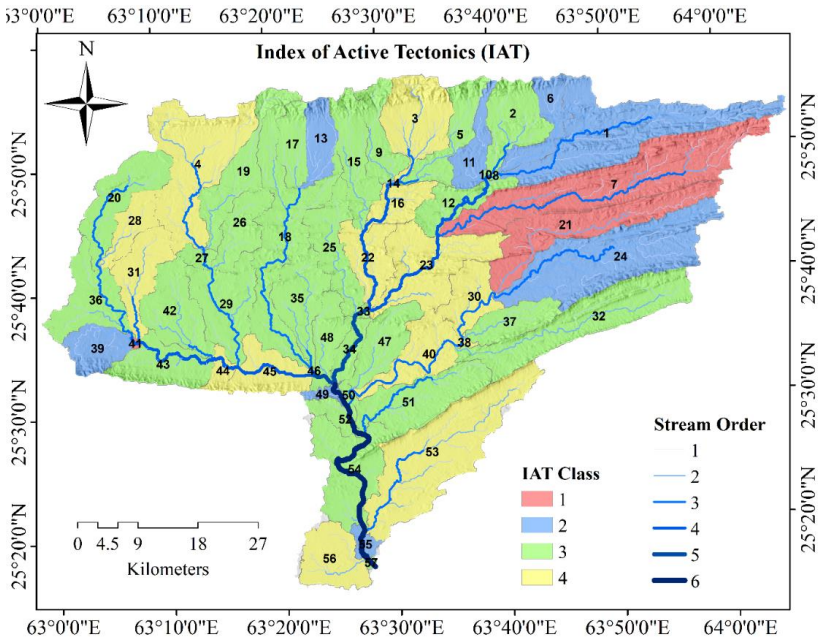

Fig. 5 Map demonstrating the calculated four IN classes of the Shadi Kaur catchment, Pasni, Balochistan-Pakistan.

Table 2. The calculated Knickpoint of the Shadi Kaur Catchment, Pasni, Balochistan-Pakistan

KP ID	Basin	Magnitude	Elevation	Distance up	Area km^2	Remarks
1	7	30.61	308	99154.57	187.67	Vertical-step knickpoint
2	32	29.36	275	90678.79	19.01	Vertical-step knickpoint
3	1	25.32	890	141371.58	17.70	Slope-break knickpoint
4	19	24.36	534	110622.90	16.20	Vertical-step knickpoint
5	1	21.99	956	143349.02	14.53	Slope-break knickpoint
6	3	23.55	587	99729.89	15.86	Vertical-step knickpoint
7	21	22.08	226	93879.40	106.63	Vertical-step knickpoint
8	3	20.24	630	100888.25	13.98	Vertical-step knickpoint

The NE-SW trending Nai Rud fault and major lineation to the northeast are linked to drainage basins with high relative tectonic activity, and so appear to have a significant impact on the landscape. However, the results do not appear to be fully independent of the lithology of the bedrock. The geomorphic indices examined in the Shadi Kaur Catchment; drainage basins primarily composed of Oligocene to Early Miocene sandstones are influenced by fault activities. Whereas, the subbasins falling in post-Miocene are primarily less resistant to erosional processes appear to have less neotectonic activities.

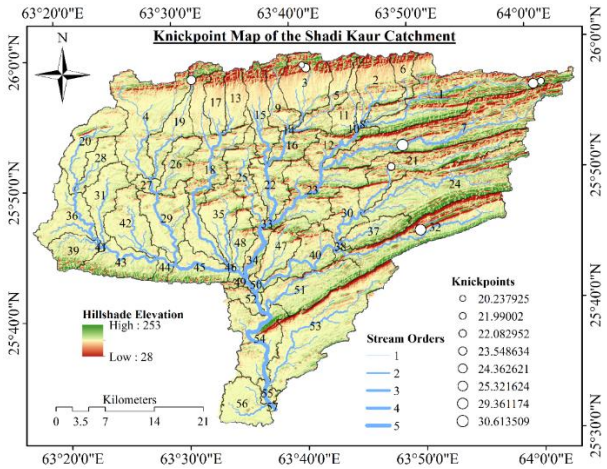

Fig. 6 Map symbolizing the hillshade map with Knick points values of the Shadi Kaur Catchment, Pasni, and Balochistan-Pakistan.

Only eight Knick points were found within six sub basins of Shadi Kaur Catchment. The location of extracted Knick points is shown in Fig. 6 which were only observed in the northern and northeastern segments. The Knick point intensities are shown in elevation vs. distance profile (Fig. 7) and range from 20.24 to 30.61 (Table 2).

The dramatic impacts and secondary conditions such as local uplift, climatic condition, erosion, accretion, etc., may categorize the Knick points into slope-break and vertical step Knick points. A slope-break Knick point divides the downstream incision from the upstream channel, which has yet to respond to boundary conditions changes. When such Knick points are formed by a single base-level decline, they move at the same retrogression rate proportional to the upstream area, resulting in Knick points of different rivers being at the same altitude (Berlin and Anderson, 2007; Crosby and Whipple, 2006). On a bounding fault, however, where many rivers cross a single structure, the elevation of Knick points can scale with fault slide rate (Boulton and Whittaker, 2009; Whittaker and Boulton, 2012). Slope-break Knick points can be formed by increased tectonic movement, such as faulting or increased slip on a fault, and can imply local uplift. Whereas, A vertical-step Knick point is associated with a shift in bedrock strength that occurs at a lithological barrier where upstream migration is restricted (Wang et al., 2015; Whipple et al., 2013). The channel is separated into upper and lower portions, despite the fact that the Knick points generated by lithological changes are frequently regarded fixed. Ksn, on the other hand, varies little or not at all throughout the Knick points. The vertical-step Knick points are regarded as climatic induced Knick points. The examined two KPs of sub basin 1 express slope-break KPs due to the streams crossing a mono-structure namely Panjgur Formation. In addition, KPs are generated by a single base-level fall and migrating to identical retrogression rates proportional to the upstream areas (Fig. 7). Thus, the KPs present in sub basin 1 are possibly initiated by local uplift and are considered to be tectonic induced. Whereas, the remaining 6 KPs of five sub basins represent vertical-step KPs because of the streams crossing poly-structures within the sub basins (Fig. 1 and Fig. 6). These changes in lithological strength produced limited migration of KPs to upstream (Fig. 7). Therefore, the KPs found in sub basins 3, 7, 19, 21, and 32 have probably generated by sea-level fall and/or climatic induced KPs.

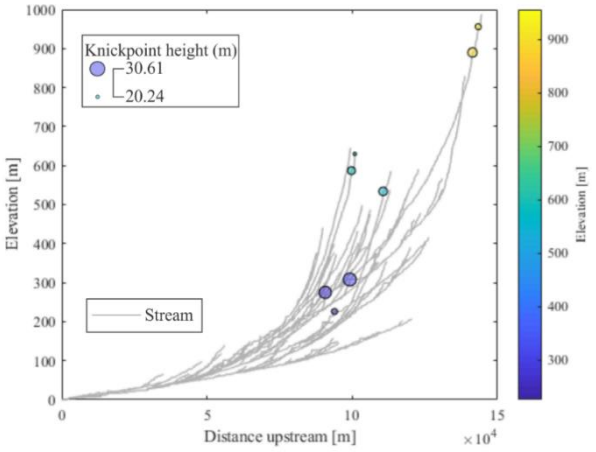

Fig. 7 Graph representing the Knick points on an elevation vs. distance upstream profile of the Shadi Kaur Catchment, Pasni, Balochistan-Pakistan.

Conclusion

Appraisal of the neotectonic activity in Shadi Kaur Catchment lead towards the following thematic points as conclusion

The IN index indicated a moderate to low level of Neotectonic activity in Shadi Kaur Catchment.
Based on lithological impacts, the drainage basins primarily composed of Oligocene to Early Miocene sandstones are influenced by fault activities, while the Late Miocene and younger areas are less resistant to erosional processes and appeared to have less Neotectonic activities. The two slope-break Knick points found in NE possibly initiated by local uplift and are considered to be tectonically induced. Whereas, the remaining six Knick points represented vertical-step due to change in lithological strength which produced limited migration of Knick points to upstream, and may have generated by sea-level fall and/or climatically induced Knick points.

References

Anand, A. K., Pradhan, S. P. (2019). Assessment of active tectonics from geomorphic indices and morphometric parameters in part of Ganga basin. *Journal of Mountain Science*, **16** (8), 1943–1961. https://doi.org/10.1007/s11629-018-5172-2

Arian, M., Aram, Z. (2014). Relative tectonic activity classification in the Kermanshah area, western Iran. *Solid Earth*, **5** (2), 1277–1291. https://doi.org/10.5194/se-5-1277-2014

Berlin, M. M., Anderson, R. S. (2007). Modeling of knickpoint retreat on the Roan Plateau, western Colorado. *Journal of Geophysical Research*, **112** (F3), F03S06. https://doi.org/10.1029/2006JF000553

Boulton, S. J., Whittaker, A. C. (2009). Quantifying the slip rates, spatial distribution and evolution of active normal faults from geomorphic analysis: Field examples from an oblique-extensional graben, southern Turkey. *Geomorphol ogy*, *104*(3–4), 299–316. https://doi.org/10.1016/j.geomorph.2008.09.007

Bull, W. B., McFadden, L. D. (1977). Tectonic geomorphology north and south of the Garlock fault, California. In: Doehring, D.O. (Ed.), Geomorphology in Arid Regions. *Proceedings of the Eighth Annual Geomorphology Symposium*, 115–138.

Cheema, M. R., Raza, S. M., Ahmed, H. (1977). Cenozoic. *Stratigraphy of Pakistan*, 56–98.

Crosby, B. T., Whipple, K. X. (2006). Knickpoint initiation and distribution within fluvial networks: 236 waterfalls in the Waipaoa River, North Island, New Zealand. *Geomorphology*, **82** (1–2), 16–38. https://doi.org/10.1016/j.geomorph.2005.08.023

Dehbozorgi, M., Pourkermani, M., Arian, M., Matkan, A. A., Motamedi, H., Hosseiniasl, A. (2010). Quantitative analysis of relative tectonic activity in the Sarvestan area, central Zagros, Iran. *Geomorphology*, **121** (3–4), 329–341. https://doi.org/10.1016/j.geomorph.2010.05.002

Douglas W. Burbank, Robert S. Anderson. (2012). *Tectonic Geomorphology* (2nd ed.). Wiley-Blackwell.

El Hamdouni, R., Irigaray, C., Fernandez, T., Chacon J., Keller, E. A. (2008). Assessment of relative active tectonics, southwest border of Sierra Nevada (Southern Spain). *Geomorphology*, **96**, 150–173.

Farhoudi, G., Karig, D. E. (1977). Makran of Iran and Pakistan as an active arc system. *Geology*, **5** (11), 664. https://doi.org/10.1130/0091-7613(1977)5<664: MOIAPA>2.0.CO; 2

Flint, J. J. (1974). Stream gradient as a function of order, magnitude, and discharge. *Water Resources Research*, **10** (5), 969–973. https://doi.org/10.1029/WR010i005p00969

Gilbert, G. K. (1877). *Geology of the Henry mountains*. Government Printing Office. Washin gton, D.C. United States. (pp. i-160). DOI: 10.3133/70038096

Goldsworthy, M., Jackson, J. (2000). Active normal fault evolution in Greece revealed by geomorphology and drainage patterns. *Journal of the Geological Society*, *157*(5), 967–981. https://doi.org/10.1144/jgs.157.5.967

Hack, J. T. (1973). Stream-profile analysis and stream-gradient index. *Journal of Research of the U.S. Geological Survey*, **1** (4), 421–429.

Harms, J. C., Cappel, H. N., Francis, D. C. (1982, February 9). Geology and Petroleum Potential of the Makran Coast, Pakistan. *All Days*. https://doi.org/10.2118/10423-MS

Harms J.C., Cappel H.N., Francis D.C. (1984). The Makran coast of Pakistan: its stratigraphy and hydrocarbon potential. In *Marine Geology and Oceanography of Arabian Sea and Coastal Pakistan* (pp. 3–26). Van Nostrand Reinhold.

Harris, I., Osborn, T. J., Jones, P., Lister, D. (2020). Version 4 of the CRU TS monthly high-resolution gridded multivariate climate dataset. *Scientific Data*, **7** (1), 109. https://doi.org/10.1038 /s41597-020-0453-3

Howard, A. D. K. G. (1983). Channel changes in badlands. *Geological Society of America Bulletin*,

94 (6), 739. https://doi.org/10.1130/0016-7606 (1983)94<739: CCIB>2.0.CO; 2

Hunting Survey Corporation. (1960). *Reconnaissance geology of part of West Pakistan: a Colombo Plan Cooperative Project*. Government of Canada for the Government of Pakistan.

Karymbalis, E., Ferentinou, M., Giles, P. T. (2018). Use of morphometric variables and self-organizing maps to identify clusters of alluvial fans and catchments in the north Peloponnese, Greece. *Geological Society, London, Special Publications*, **440** (1), 45–64. https://doi.org/10.1144/SP440.7

Karymbalis, E., Papanastassiou, D., Gaki-Papanastassiou, K., Ferentinou, M., Chalkias, C. (2016). Late Quaternary rates of stream incision in Northeast Peloponnese, Greece. *Frontiers of Earth Science*, **10** (3), 455–478. https://doi.org/10.1007/s11707-016-0577-0

Kehl, M. (2009). Quaternary climate change in Iran – the state of knowledge. *ERDKUNDE*, **63** (1), 1–17. https://doi.org/10.3112/erdkunde.2009.01.01

Keller, E. A., Pinter, N. (2002). *Active Tectonics: Earthquakes, Uplift, and Landscape*. Prentice Hall, Upper Saddle River, N. J.

Khan, W., Dost, C., Murad, F., Muhammad, A., Ahmad, F. (2022). Neotectonic Activity in Quetta-Ziarat Region, Northwest Quetta City, Pakistan. *International Journal of Economic and Environmental Geology*, **13** (4), 24-28.

Khan, W., and Mirwani, M. (2020). Probing the nature and characteristics of active mud volcanic clusters in Makran coastal zone, Pakistan. International Journal of Research - Granthaalayah, 8(3), 214-222. https://doi.org/10.29121/granthaalayah.v8.i3.2020.145.

Khan, W., Zhang, K., Liang, H., Yu, P. (2023)a. Geochemical Assessment of River Sediments at the Outlets of Eastern Makran, Pakistan; Implications for Source Area Weathering and Provenance. *Minerals*, **13** (3), 348. https://doi.org/10.3390/min13030348

Khan, W., Zhang, K., Liang, H., & Yu, P. (2023)b. Provenance for the Makran Flysch Basin in Pakistan: Implications for interaction between the Indian, Eurasian, and *Arabian plates. Journal of Asian Earth Sciences*, **248**, 105626. https://doi.org/10.1016/j.jseaes.2023.105626

Kirby, E., Whipple, K. (2001). Quantifying differential rock-uplift rates via stream profile analysis. *Geology*, *29*(5), 415. https://doi.org/10.1130/0091-7613(2001)029<0415: QDRURV>2.0.CO; 2

Mackin, J. H. (1948). Concept of the graded river. *Bulletin of the Geological Society of America*, *59*, 463–512.

Mahmood, S. A., Gloaguen, R. (2012). Appraisal of active tectonics in Hindu Kush: Insights from DEM derived geomorphic indices and drainage analysis. *Geoscience Frontiers*, **3** (4), 407–428. https://doi.org/10.1016/j.gsf.2011.12.002

Maroukian, H., Gaki-Papanastassiou, K., Karymbalis, E., Vouvalidis, K., Pavlopoulos, K., Papanastassiou, D., & Albanakis, K. (2008). Morphotectonic control on drainage network evolution in the Perachora Peninsula, Greece. *Geomorphology*, **102** (1), 81–92. https://doi.org/10.1016/j.geomorph.2007.07.021

Mayer, L. (1990). *Introduction to Quantitative Geomorphology*. Prentice Hall, Englewood, Cliffs, NJ.

Nairui Wang, Zhiyong Han, Xusheng Li, Gang Chen, Xianyan Wang, Huayu Lu. (2015). Tectonic uplift of Mt. Lushan indicated by the steepness indices of the river longitudinal profiles. *Acta Geographica Sinica*, **70** (9), 1516–1525.

Piacentini, D., Troiani, F., Servizi, T., Nesci, O., Veneri, F. (2020). SLiX: A GIS Toolbox to Support Along-Stream Knickzones Detection through the Computation and Mapping of the Stream Length-Gradient (SL) Index. *ISPRS International Journal of Geo-Information*, 9 (2), 69. https://doi.org/10.3390/ijgi9020069

Pike, R. J., & Wilson, S. E. (1971). Elevation-relief ratio, hypsometric integral, and geomorphic area altitude analysis. *GSA Bulletin*, *82*(4), 1079–1084.

Siddiqui, S., Soldati, M. (2014). Appraisal of active tectonics using DEM-based hypsometric integral and trend surface analysis in Emilia-Romagna Apennines, northern Italy. *Turkish Journal of Earth Sciences*, **23**, 277–292. https://doi.org/10.3906/yer-1306-12

Strahler, A. N. (1952). Hypsometric (area-altitude) analysis of erosional topography. *Geological Society of America Bulletin*, **63** (11), 1117–1142.

Tucker, G. E., Whipple, K. X. (2002). Topographic outcomes predicted by stream erosion models: Sensitivity analysis and intermodel comparison. *Journal of Geophysical Research: Solid Earth*, *107*(B9), ETG 1-1-ETG 1-16. https://doi.org/10.1029/2001JB000162

Vassilakis E, Skourtsos E, Kranis H. (2007). Tectonic uplift rate estimation with the quantification of morphometric indices. *8th Panhellenic Geographical Congress*, 17–26.

Whipple, K. X., DiBiase, R. A., Crosby, B. T. (2013). Bedrock Rivers. **In** *Treatise on Geomorphology* (pp. 550–573). Elsevier. https://doi.org/10.1016/B978-0-12-374739-6.00254-2

Whittaker, A. C., Boulton, S. J. (2012). Tectonic and climatic controls on Knickpoint retreat rates and landscape response times. *Journal of Geophysical Research: Earth Surface*, **117** (F2). https://doi.org/10.1029/2011JF002157

Wobus, C., Whipple, K. X., Kirby, E., Snyder, N., Johnson, J., Spyropolou, K., Crosby, B., Sheehan, D. (2006). Tectonics from topography: Procedures, promise, and pitfalls. In *Tectonics, Climate, and Landscape Evolution*, 55–74. Geological Society of America. https://doi.org/10.1130/2006.2398(04).